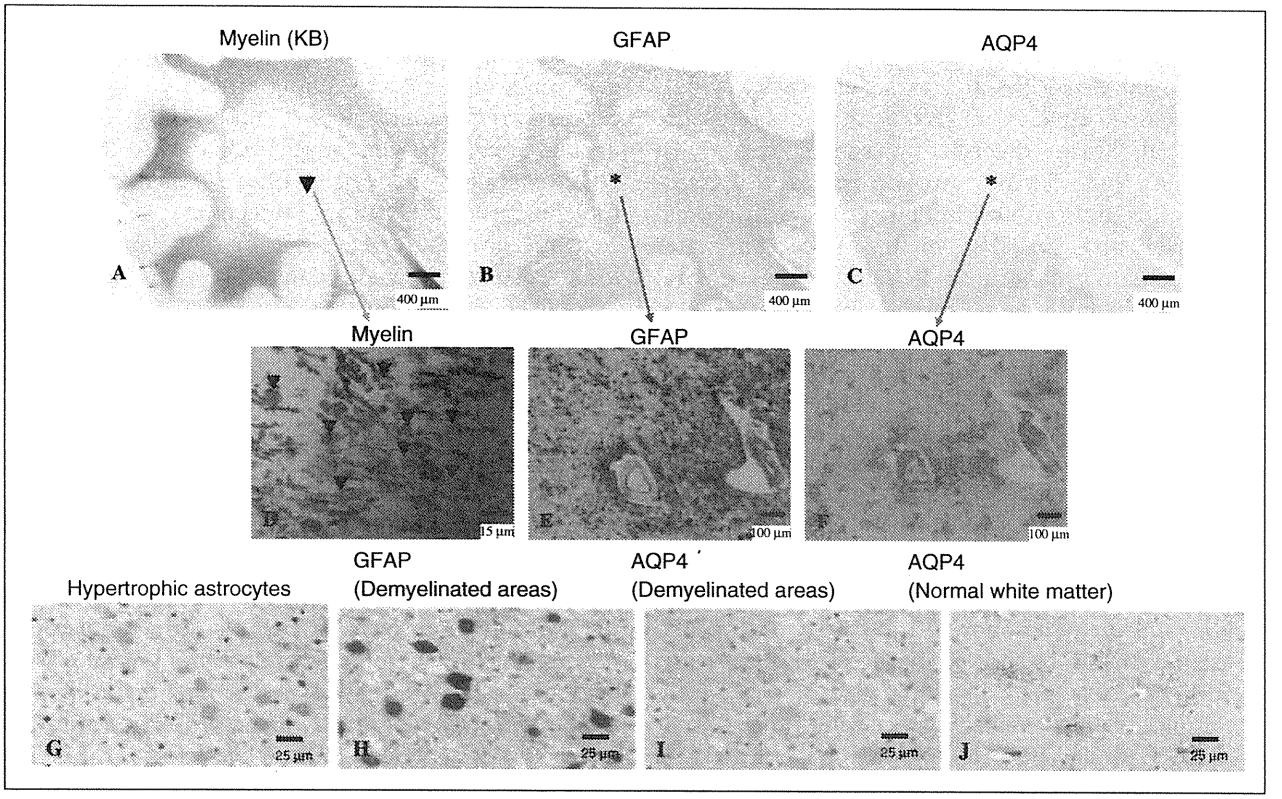

Figure 1. Extensive aquaporin-4 loss in the demyelinated and preserved myelin layers in Baló's concentric sclerosis lesions. (A) The cerebral white matter shows concentric demyelinated lesions. (B) GFAP is expressed in the lesion center, but not in the lamellar necrotic foci at the lesion edge (arrows). (C) AQP4 immunoreactivity is largely lost in the lesion center, with lamellar myelin-staining patterns. (D) Dense infiltration of foamy macrophages phagocytosing myelin debris in the demyelinating layer. (E) Astrocytes strongly express GFAP. (F) Astrocytes lack surface staining for AQP4. (G) Numerous reactive, hypertrophic astrocytes are seen, both in the demyelinated and in the preserved myelin layers. (H) Hypertrophic astrocytes are strongly stained for GFAP. (I) AQP4 is totally lost in hypertrophic astrocytes. (J) Non-reactive astrocytes show AQP4 staining on the cell surface and on their processes in the unaffected white matter, with preserved myelin staining and no inflammatory infiltration. A, D, KB staining; B, E, H, GFAP immunohistochemistry (IHC); C, F, I, J, AQP4 IHC. AQP4 = aquaporin-4; GFAP = glial fibrillary acidic protein; KB = Klüver-Barrera staining. Reproduced in part from Matsuoka et al. *Acta Neuropathologica* 2010; 120: 651–660, with permission.

(Figures 2 and 3). Thereby, concentric rings are formed step by step. However, as mentioned above, Baló's disease frequently shows a concentric lamellar pattern at the time of initial presentation on MRI. Apparently, successive formation of concentric rings by alternating layers of apoptotic oligodendrocytes and preconditioned oligodendrocytes cannot account for the simultaneous emergence of concentric rings in Baló's disease. Extensive AQP4 loss in the demyelinated as well as in the myelinated layers of Baló's concentric rings prompted us to consider astrocytopathy to be upstream of oligodendrogliopathy. Previously reported close contact of hypertrophic astrocytes with oligodendrocytes in the demyelinated layers of Baló's lesions may suggest a possibility that abnormal interaction between these two cell types may lead to oligodendroglial damage followed by extensive demyelination.

At present, we do not know the mechanism of AQP4 loss in the hypertrophic astrocytes in Baló's lesions. In NMO, antibody-mediated killing of astrocytes is proposed. In a rat model of autoimmune encephalomyelitis (EAE), induced by the transfer of myelin basic protein (MBP)-specific T cells, IgG containing anti-AQP4 antibody from IgG-seropositive NMO patients reproduces astrocyte loss in vivo.[48–50] However, no disease or neuropathological CNS alterations were observed when AQP4 antibody was injected into young rats with a leaky BBB, or after transfer of non-encephalitogenic T cells.[50] Thus, anti-AQP4 antibody is pathogenic to the CNS in an inflammatory state. By contrast, such a mechanism cannot be operating in Baló's disease, because there exists neither vasculocentric deposition of immunoglobulin and complement in the lesions nor anti-AQP4 antibody in sera. Since T-cell infiltration

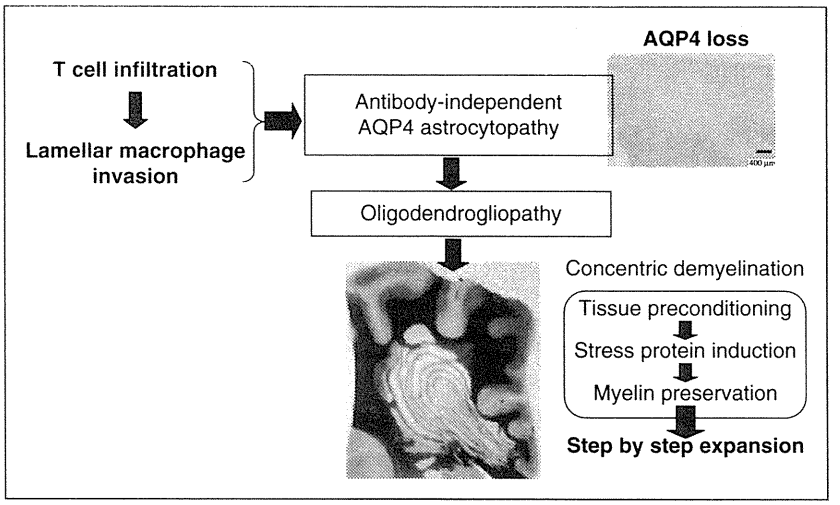

Figure 2. Hypothetical cascade of events in Baló's disease.

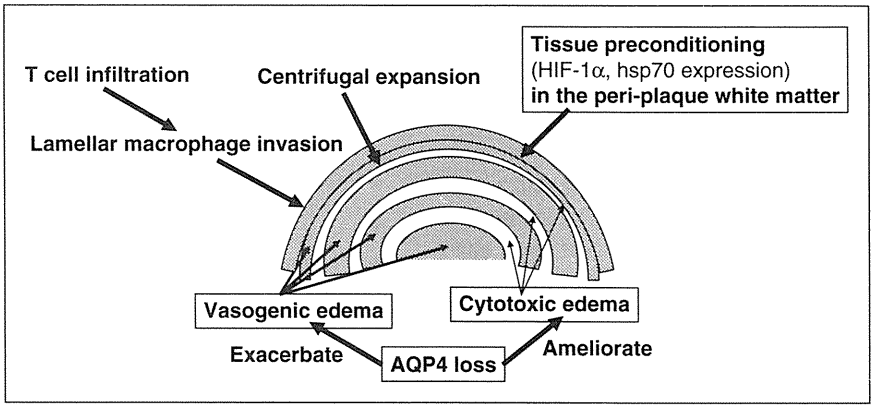

Figure 3. Hypothetical mechanisms for Baló's concentric ring formation.

and macrophage invasion appear to herald development of astrocytopathy and oligodendrogliopathy/demyelination, these immunocytes may induce down-modulation of AQP4 through the actions of inflammatory products. Alternatively, because AQP4 is down-regulated in hypoxic conditions and in the ischemic core at the acute stage,[51–54] vessel obliteration or mitochondrial impairment associated with heavy lymphocytic inflammation may lead to tissue hypoxia, which, in turn, may induce AQP4 down-regulation. The notion that hypoxia-like tissue injury is operative in Baló's concentric sclerosis[19] further supports such a mechanism.

In Baló's disease, very early lesions could be cytotoxic edema, and alternating layers of cytotoxic and vasogenic edema may develop in association with lamellar infiltration of inflammatory cells, which is inferred by concentric or serpentine enhancement of the lesions with contrast media and by alternating bands of increased and restricted diffusion on ADC maps. In AQP4 knockout mice, a prolongation of vasogenic edema,[55] but a decrease in the level of cytotoxic edema[56] was noted and EAE was markedly attenuated.[57] Thus, AQP4 loss is not necessarily harmful in CNS inflammatory conditions. Since AQP4 loss is widespread in entire lesions in Baló's cases, such a loss may potentiate tissue destruction through prolongation of vasogenic edema on one hand, whereas it may ameliorate tissue damage via reduction of cytotoxic edema on the other, resulting in alternating bands of demyelination and preserved myelin. In anti-AQP4 antibody-positive NMO cases, antibody-mediated loss of AQP4 may exert similar influence, thereby producing lamellar rings in some NMO cases. If tissue destruction becomes severe and persistent, demyelinated bands may give rise to necrotic ones, as reported in the case of concentric lacunar leukoencephalopathy in NMO.[41] Thus, AQP4 loss and astrocytopathy may contribute to the development of lamellar demyelination, irrespective of anti-AQP4 antibody-dependent (anti-AQP4

antibody-positive NMO) or -independent conditions (Baló's disease).

Conclusions and future perspectives

The mechanism of antibody-independent AQP4 loss remains to be elucidated. The effects of plentiful inflammatory factors from T cells and macrophages on AQP4 expression in astrocytes should be further studied in vivo and in vitro. Furthermore, the mechanism of simultaneous development of lamellar inflammation in Baló's disease, which is seen pathologically and is also evident by lamellar and serpentine enhancement of the rings on MRI, remains unknown. Step-by-step outward expansion of Baló's concentric rings, together with induction of stress proteins in the outer, normal-appearing white matter, seems to explain only a fraction of the cases with this condition or a later phase of the disease. Increasing evidence suggests that Th17 cells, but not Th1 cells, are responsible for organ-specific autoimmune diseases such as EAE.[58,59] Th17 cells carrying granzyme B have recently been shown to efficiently disrupt BBB tight junctions and loosen the BBB.[60] Therefore, autoimmune Th17 cells may initiate BBB disruption and inflammation in demyelinating disease. Such cell-mediated inflammatory components could also be an important area for future research into Baló's disease, no matter what the target CNS antigens are. I believe that the discovery of antibody-independent AQP4 astrocytopathy opens an intriguing field of research in Baló's disease, and that Baló's disease could be a possible link between MS and NMO, both of which can develop concentric rings of Baló. This hypothesis is based on descriptive data and it should be tested by future experimental studies.

Acknowledgments

I thank Drs Takeshi Matsuoka, Satoshi O Suzuki, Katsuhisa Masaki, Noriko Isobe, Tomomi Yonekawa and Takuya Matsushita for their help with neuropathological and immunological examinations.

Funding

This research received no specific grant from any funding agency in the public, commercial, or not-for-profit sectors.

Conflict of interest statement

None declared.

References

1. Marburg O. Die so-genannte 'akute multiple Sklerose' (Encephalomyelitis periaxialis scleroticans). *Jahrb Psychiatr* 1906; 28: 213–312.
2. Baló J. Encephalitis periaxialis concentrica. *Arch Neurol Psychiatry* 1928; 19: 242–264.
3. Matsuoka T, Suzuki SO, Iwaki T, Tabira T, Ordinario AT and Kira JI. Aquaporin-4 astrocytopathy in Balo's disease. *Acta Neuropathol* 2010; 120: 651–660.
4. Kuroiwa Y. Concentric sclerosis. In: Koetsier JC (ed.) *Handbook of clinical neurology. Demyelinating disease.* Amsterdam: Elsevier, 1985, pp.409–417.
5. Courville CB. Concentric sclerosis. In: Vinken PJ, Bruyn GW (eds) *Handbook of clinical neurology. Multiple sclerosis and other demyelinating diseases.* Amsterdam: Elsevier, 1970, pp.437–451.
6. Bolay H, Karabudak R, Tacal T, Önol B, Selekler K and Saribas SO. Baló's concentric sclerosis. Report of two patients with magnetic resonance imaging follow-up. *J Neuroimaging* 1996; 6: 98–103.
7. Moore GR, Berry K, Oger JF, Prout AE, Graeb DA and Nugent RA. Baló's concentric sclerosis: surviving normal myelin in a patient with a relapsing-remitting clinical course. *Mult Scler* 2001; 7: 375–382.
8. Karaarslan E, Altintas A, Senol U, et al. Baló's concentric sclerosis: clinical and radiologic features of five cases. *AJNR Am J Neuroradiol* 2001; 22: 1362–1367.
9. Anschel DJ. Reply to the paper by Wiendl et al.: diffusion abnormality in Balo's concentric sclerosis: clues for the pathogenesis. *Eur Neurol* 2006; 55: 111–112.
10. Lindquist S, Bodammer N, Kaufmann J, et al. Histopathology and serial, multimodal magnetic resonance imaging in a multiple sclerosis variant. *Mult Scler* 2007; 13: 471–482.
11. Wang C, Zhang KN, Wu XM, et al. Baló's disease showing benign clinical course and co-existence with multiple sclerosis-like lesions in Chinese. *Mult Scler* 2008; 14: 418–424.
12. Iannucci G, Mascalchi M, Salvi F and Filippi M. Vanishing Balò-like lesions in multiple sclerosis. *J Neurol Neurosurg Psychiatry* 2000; 69: 399–400.
13. Adams RD and Kubik CS. The morbid anatomy of the demyelinative diseases. *Am J Med* 1952; 12: 510–546.
14. Makifuchi T. Pathology of concentric sclerosis of Baló's disease. *Neurol Med* 2002; 56: 498–501. (Japanese).
15. Moore GRW, Neumann PE, Suzuki K, Lijtmaer HN, Traugott U and Raine CS. Balo's concentric sclerosis: new observations on lesion development. *Ann Neurol* 1985; 17: 604–611.
16. Kreft KL, Mellema SJ and Hintzen RQ. Spinal cord involvement in Balo's concentric sclerosis. *J Neurol Sci* 2009; 279: 114–117.
17. Yao DL, Webster Hde F, Hudson LD, et al. Concentric sclerosis (Balo): morphometric and in situ hybridization study of lesions in six patients. *Ann Neurol* 1994; 35: 18–30.
18. Lucchinetti C, Brück W, Parisi J, Scheithauer B, Rodriguez M and Lassmann H. Heterogeneity of multiple sclerosis lesions: implications for the pathogenesis of demyelination. *Ann Neurol* 2000; 47: 707–717.
19. Lassmann H. Hypoxia-like tissue injury as a component of multiple sclerosis lesions. *J Neurol Sci* 2003; 206: 187–191.
20. Stadelmann C, Ludwin S, Tabira T, et al. Tissue preconditioning may explain concentric lesions in Baló's type of multiple sclerosis. *Brain* 2005; 128: 979–987.

21. Kishimoto R, Yabe I, Niino M, et al. Baló's concentric sclerosis-like lesion in the brainstem of a multiple sclerosis patient. *J Neurol* 2008; 255: 760–761.
22. Graber JJ, Kister I, Geyer H, Khaund M and Herbert J. Neuromyelitis optica and concentric rings of Baló in the brainstem. *Arch Neurol* 2009; 66: 274–275.
23. Chen CJ, Chu NS, Lu CS and Sung CY. Serial magnetic resonance imaging in patients with Balò's concentric sclerosis: natural history of lesion development. *Ann Neurol* 1999; 46: 651–656.
24. Kastrup O, Stude P and Limmroth V. Balo's concentric sclerosis. Evolution of active demyelination demonstrated by serial contrast-enhanced MRI. *J Neurol* 2002; 249: 811–814.
25. Wiendl H, Weissert R, Herrlinger U, Krapf H and Küker W. Diffusion abnormality in Balo's concentric sclerosis: clues for the pathogenesis. *Eur Neurol* 2005; 53: 42–44.
26. Kavanagh EC, Heran MKS, Fenton DM, Lapointe JS, Nugent RA and Graeb DA. Diffusion-weighted imaging findings in Balo concentric sclerosis. *Br J Radiol* 2006; 79: e28–e31.
27. Schaefer PW. Applications of DWI in clinical neurology. *J Neurol Sci* 2001; 186(Suppl 1): S25–S35.
28. Mader I, Herrlinger U, Klose U, Schmidt F and Küker W. Progressive multifocal leukoencephalopathy: analysis of lesion development with diffusion-weighted MRI. *Neuroradiology* 2003; 45: 717–721.
29. Küker W, Ruff J, Gaertner S, Mehnert F, Mäder I and Nagele T. Modern MRI tools for the characterization of acute demyelinating lesions: value of chemical shift and diffusion-weighted imaging. *Neuroradiology* 2004; 46: 421–426.
30. Muir KW, Buchan A, von Kummer R, Rother J and Baron JC. Imaging of acute stroke. *Lancet Neurol* 2006; 5: 755–768.
31. Balasubramanya KS, Kovoor JME, Jayakumar PN, et al. Diffusion-weighted imaging and proton MR spectroscopy in the characterization of acute disseminated encephalomyelitis. *Neuroradiology* 2007; 49: 177–183.
32. Castriota-Scanderbeg A, Sabatini U, Fasano F, et al. Diffusion of water in large demyelinating lesions: a follow-up study. *Neuroradiology* 2002; 44: 764–767.
33. Rovira A, Pericot I, Alonso J, Rio J, Grivé E and Montalban X. Serial diffusion-weighted MR imaging and proton MR spectroscopy of acute large demyelinating brain lesions: case report. *AJNR Am J Neuroradiol* 2002; 23: 989–994.
34. Rosso C, Remy P, Creange A, Brugieres P, Cesaro P and Hosseini H. Diffusion-weighted MR imaging characteristics of an acute strokelike form of multiple sclerosis. *AJNR Am J Neuroradiol* 2006; 27: 1006–1008.
35. Balashov KE, Aung LL, Dhib-Jalbut S, Keller IA. Acute multiple sclerosis lesion: conversion of restricted diffusion due to vasogenic edema. *J Neuroimaging* 2009 (accessed 28 January 2011).
36. Pichiecchio A, Tavazzi E, Maccabelli G, et al. What insights have new imaging techniques given into aggressive forms of MS -different forms of MS or different from MS? *Mult Scler* 2009; 15: 285–293.
37. Przeklasa-Auth M, Ovbiagele B, Yim C and Shewmon DA. Multiple sclerosis with initial stroke-like clinicoradiologic features: case report and literature review. *J Child Neurol* 2010; 25: 732–737.
38. Malhotra HS, Jain KK, Agarwal A, et al. Characterization of tumefactive demyelinating lesions using MR imaging and in-vivo proton MR spectroscopy. *Mult Scler* 2009; 15: 193–203.
39. Chen CJ. Serial proton magnetic resonance spectroscopy in lesions of Balo concentric sclerosis. *J Comput Assist Tomogr* 2001; 25: 713–718.
40. Field EJ, Miller H and Russell DS. Observations on glial inclusion bodies in a case of acute disseminated sclerosis. *J Clin Pathol* 1962; 15: 278–284.
41. Currie S, Roberts AH and Urich H. The nosological position of concentric lacunar leucoencephalopathy. *J Neurol Neurosurg Psychiatry* 1970; 33: 131–137.
42. Itoyama Y, Tateishi J and Kuroiwa Y. Atypical multiple sclerosis with concentric or lamellar demyelinated lesions: two Japanese patients studied post mortem. *Ann Neurol* 1985; 17: 481–487.
43. Lennon VA, Wingerchuk DM, Kryzer TJ, et al. A serum autoantibody marker of neuromyelitis optica: distinction from multiple sclerosis. *Lancet* 2004; 364: 2106–2112.
44. Lennon VA, Kryzer TJ, Pittock SJ, Verkman AS and Hinson SR. IgG marker of optic-spinal multiple sclerosis binds to the aquaporin-4 water channel. *J Exp Med* 2005; 202: 473–477.
45. Misu T, Fujihara K, Kakita A, et al. Loss of aquaporin 4 in lesions of neuromyelitis optica: distinction from multiple sclerosis. *Brain* 2007; 130: 1224–1234.
46. Roemer SF, Parisi JE, Lennon VA, et al. Pattern-specific loss of aquaporin-4 immunoreactivity distinguishes neuromyelitis optica from multiple sclerosis. *Brain* 2007; 130: 1194–1205.
47. Masaki K, Matsuoka T, Suzuki SO, et al. Extensive aquaporin-4 (AQP4) loss in Balo's concentric sclerosis in the absence of anti-AQP4 antibody. (Abstract) *Mult Scler* 2010 (in press).
48. Kinoshita M, Nakatsuji Y, Kimura T, et al. Neuromyelitis optica: passive transfer to rats by human immunoglobulin. *Biochem Biophys Res Commun* 2009; 386: 623–627.
49. Bennett JL, Lam C, Kalluri SR, et al. Intrathecal pathogenic anti-aquaporin-4 antibodies in early neuromyelitis optica. *Ann Neurol* 2009; 66: 617–629.
50. Bradl M, Misu T, Takahashi T, et al. Neuromyelitis optica: pathogenicity of patient immunoglobulin in vivo. *Ann Neurol* 2009; 66: 630–643.
51. Frydenlund DS, Bhardwaj A, Otsuka T, et al. Temporary loss of perivascular aquaporin-4 in neocortex after transient middle cerebral artery occlusion in mice. *Proc Natl Acad Sci U S A* 2006; 103: 13532–13536.
52. Fujita Y, Yamamoto N, Sobue K, et al. Effect of mild hypothermia on the expression of aquaporin family in cultured rat astrocytes under hypoxic condition. *Neurosci Res* 2003; 47: 437–444.
53. Lee M, Lee SJ, Choi HJ, et al. Regulation of AQP4 protein expression in rat brain astrocytes: role of P2X7 receptor activation. *Brain Res* 2008; 1195: 1–11.

54. Meng S, Qiao M, Lin L, Del Bigio MR, Tomanek B and Tuor UI. Correspondence of AQP4 expression and hypoxic-ischaemic brain oedema monitored by magnetic resonance imaging in the immature and juvenile rat. *Eur J Neurosci* 2004; 19: 2261–2269.
55. Papadopoulos MC, Manley GT, Krishna S and Verkman AS. Aquaporin-4 facilitates reabsorption of excess fluid in vasogenic brain edema. *FASEB J* 2004; 18: 1291–1293.
56. Manley GT, Fujimura M, Ma T, et al. Aquaporin-4 deletion in mice reduces brain edema after acute water intoxication and ischemic stroke. *Nat Med* 2000; 6: 159–163.
57. Li L, Zhang H and Verkman AS. Greatly attenuated experimental autoimmune encephalomyelitis in aquaporin-4 knockout mice. *BMC Neurosci* 2009; 10: 94.
58. Cua DJ, Sherlock J, Chen Y, et al. Interleukin-23 rather than interleukin-12 is the critical cytokine for autoimmune inflammation of the brain. *Nature* 2003; 421: 744–748.
59. Weaver CT, Hatton RD, Mangan PR and Harrington LE. IL-17 family cytokines and the expanding diversity of effector T cell lineages. *Annu Rev Immunol* 2007; 25: 821–852.
60. Kebir H, Kreymborg K, Ifergan I, et al. Human TH17 lymphocytes promote blood-brain barrier disruption and central nervous system inflammation. *Nat Med* 2007; 13: 1173–1175.

MULTIPLE SCLEROSIS JOURNAL | MSJ

Multiple Sclerosis Journal
17(7) 885–887

DOI: 10.1177/1352458510391690
msj.sagepub.com
SAGE

Wall-eyed bilateral internuclear ophthalmoplegia (WEBINO) syndrome in a patient with neuromyelitis optica spectrum disorder and anti-aquaporin-4 antibody

Koji Shinoda[1], Takuya Matsushita[2], Konosuke Furuta[1], Noriko Isobe[1], Tomomi Yonekawa[1], Yasumasa Ohyagi[1] and Jun-ichi Kira[1]

Abstract

This report describes, for the first time, an occurrence of wall-eyed bilateral internuclear ophthalmoplegia (WEBINO) in a 19-year-old female with neuromyelitis optica (NMO) spectrum disorder, who had anti-aquaporin-4 (AQP4) antibody. A high signal intensity lesion on T2-weighted MRI was detected in the midbrain tegmentum adjacent to the aqueduct, and presumably involved the medial longitudinal fasciculus bilaterally at the caudal levels. Plasma exchange resolved both WEBINO syndrome and the midbrain lesion. Although WEBINO syndrome is occasionally reported in multiple sclerosis patients, diagnosis of NMO should not be excluded in patients with WEBINO syndrome, because AQP4 is expressed abundantly around the periaqueductal region.

Keywords

aquaporin-4, MRI, neuromyelitis optica, WEBINO syndrome

Date received: 8th September 2010; revised: 20th October 2010; accepted: 20th October 2010

Introduction

Wall-eyed bilateral internuclear ophthalmoplegia (WEBINO) is a rarely reported syndrome. Clinically, patients with WEBINO syndrome demonstrate exotropia in the primary eye position and a bilateral adduction deficit with abducting nystagmus on horizontal gaze.[1] The causal lesions are thought to be bilateral medial longitudinal fasciculi (MLF). WEBINO syndrome has been reported in patients with cerebrovascular diseases, multiple sclerosis (MS), brainstem tumor, and supranuclear progressive palsy.[1–3] Here, for the first time, we report a patient with neuromyelitis optica (NMO) spectrum disorder (NMOSD) who had a specific anti-aquaporin-4 (AQP4) antibody[4,5] and presented with WEBINO syndrome.

Case report

A 19-year-old female was admitted to our hospital with a chief complaint of double vision for 2 days. Eight months before admission, she had been referred and admitted to our hospital because of an acute onset of double vision, dysphagia, dysarthria and right-sided weakness and paresthesia. At the first admission, her anti-nuclear antibody (ANA) and anti-SS-A antibody were positive. Anti-AQP4 antibody was also positive using an immunofluorescence assay.[6] The CSF was hypercellular (38/μl, all mononuclear cells) with slightly elevated levels of total protein (52 mg/dl) and myelin basic protein (815 pg/ml), but no oligoclonal bands were found. Her brain and spinal cord MRI revealed

[1]Department of Neurology, Neurological Institute, Graduate School of Medical Sciences, Kyushu University, Japan.
[2]Department of Clinical Neuroimmunology, Graduate School of Medical Sciences, Kyushu University, Japan.

Corresponding author:
Jun-ichi Kira, Department of Neurology, Neurological Institute, Graduate School of Medical Sciences, Kyushu University, 311 Maidashi, Higashi-ku, Fukuoka 812-8582, Japan
Email: kira@neuro.med.kyushu-u.ac.jp

hyperintense areas on T2-weighted and fluid-attenuated inversion recovery (FLAIR) images in the hypothalamus bilaterally and from the medulla to C1 in the spinal cord without contrast enhancement (Figure 1A and B). In the spinal cord, T2-weighted images revealed high signal intensity lesions at the levels C4–7 (Figure 1A), T9–10 and T12–L1. We diagnosed her as having an NMOSD due to the presence of anti-AQP4 antibody, longitudinally extensive spinal cord lesions (LESCLs) and atypical brain lesions, which collectively are considered to be characteristic of NMO. Intravenous methylprednisolone pulse therapy (1000 mg daily for 3 days) followed by oral prednisolone (50 mg/day with gradual taper) was initiated. On discharge, she had only slight hemiparesis and hypesthesia on the right side of her body and slight ataxia of all four limbs.

At the second admission, neurological examination revealed normal convergence, a sluggish light reflex, adduction deficit and exotropia of the right eye, monocular abducting nystagmus of the left eye on leftward gaze, right-side deviation on tongue protrusion and Lhermitte's sign. The CSF had minimal hypercellularity (6/μl). ANA, anti-SS-A antibody and anti-AQP4 antibody were again all positive in her serum. Methylprednisolone pulse therapy (1000 mg daily for 3 days) was administered, but there was no effect on her double vision. Additionally, an adduction deficit of the left eye and exotropia of either eye on primary

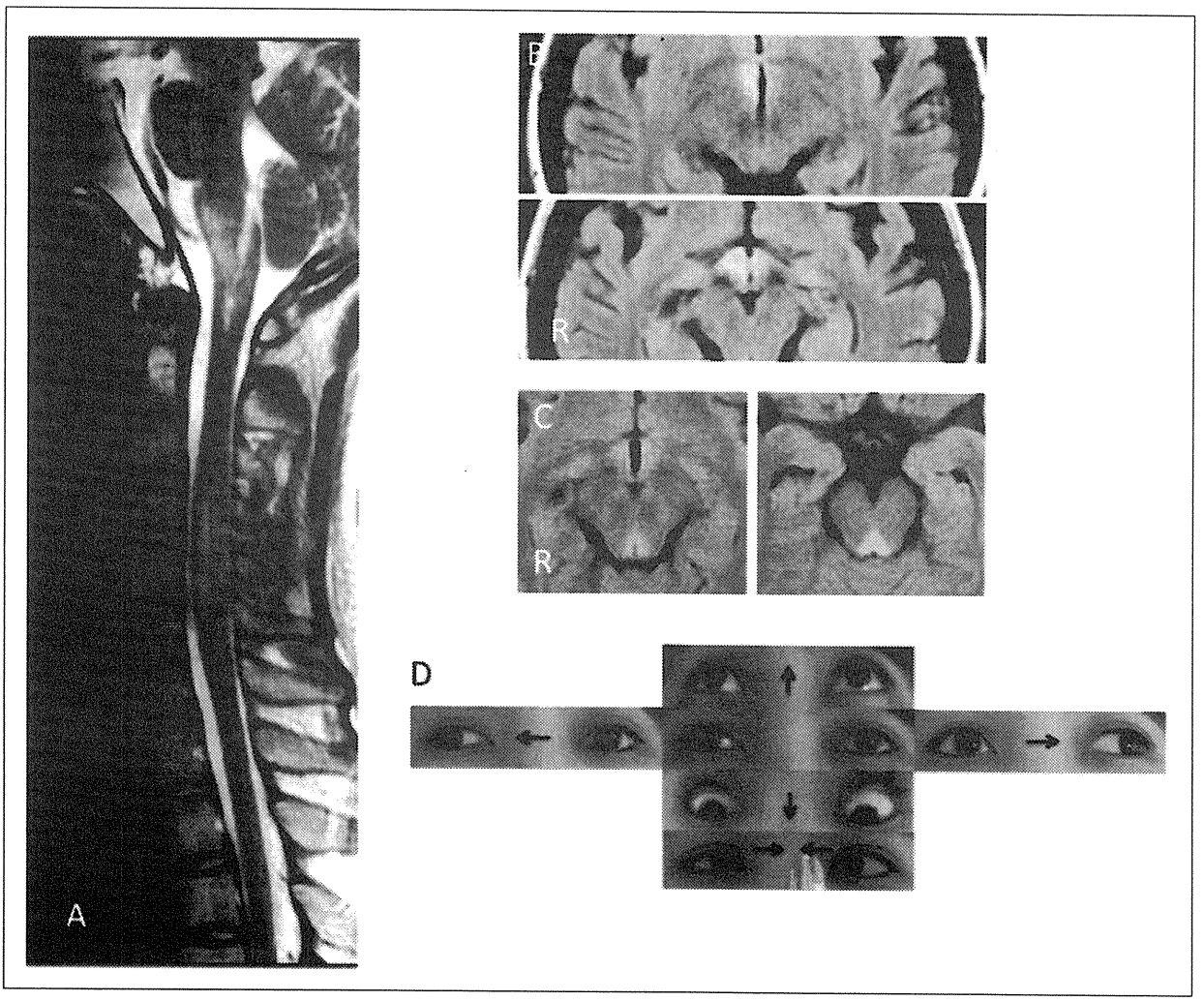

Figure 1. T2-weighted image (TR = 2500 ms, TE = 108 ms) at the first admission demonstrates a continuous hyperintense lesion from the medulla to C1, and a longitudinally extensive spinal cord lesion from C4 to C7 (**A**). FLAIR images (TR = 9000 ms, TE = 97 ms) show band-like hyperintense lesions in the hypothalamus bilaterally (B). MRI at the time of appearance of WEBINO syndrome shows a high signal intensity lesion in the midbrain tegmentum adjacent to the aqueduct on FLAIR images (TR = 9000 ms, TE = 110 ms) (**C**). Photographs of ocular movement demonstrating exotropia of either eye in the primary eye position and an adduction deficit of either eye on attempted lateral gaze (**D**). Convergence is intact. The arrows indicate the directions of attempted gaze.
FLAIR: fluid-attenuated inversion recovery, WEBINO: wall-eyed bilateral internuclear ophthalmoplegia.

gaze position occurred. At this point, she had bilateral adduction deficit with dissociated abducting nystagmus of abducting eyes on lateral gaze and exotropia of either eye (Figure 1D), which met the criteria for WEBINO syndrome.[1] Head MRI disclosed a new hyperintense lesion on T2-weighted and FLAIR images in the dorsal portion of the midbrain around the aqueduct (Figure 1C). Following corticosteroid therapy, plasma exchange was performed three times, with marked improvement of her double vision and disappearance of her exotropia.

Discussion

We report the first case of a patient with anti-AQP4 antibody displaying WEBINO syndrome. NMO consists of optic neuritis and myelitis, and is usually associated with LESCLs extending over three or more vertebral segements.[7] Initially, NMO was considered not to be accompanied by brain lesions; however, the discovery of NMO-IgG revealed that atypical brain lesions, such as bilateral diencephalic lesions, large confluent cerebral hemispheric lesions, and medullary lesions extending from the cervical cord, were not rarely encountered in this condition.[8] Although the present patient had no optic neuritis, the presence of anti-AQP4 antibody, LESCLs and atypical brain lesions, namely bilateral hypothalamic lesions and a medullary lesion extending from the C1 level of the spinal cord, strongly suggests that she was suffering from the early stage of an NMOSD.[9]

WEBINO syndrome is considered to be caused by lesions involving the bilateral MLF and medial rectus subnucleus.[1] However, it is assumed that an involvement of the oculomotor nucleus is not essential for exotropia, and that an imbalance between bilateral paramedian pontine reticular formation (PPRF) activities on eye fixation is responsible.[10] In our patient, the lesion responsible for WEBINO syndrome, as determined by MRI, is the midbrain tegmentum lesion adjacent to the aqueduct. This lesion is likely to involve the MLF near the oculomotor nucleus bilaterally.

WEBINO syndrome has repeatedly been reported in patients with MS, in which brainstem lesions involving bilateral MLF frequently develop. In patients with NMO, the periaqueductal region, where an expression of aquaporin-4 is supposed to be high,[9] is occasionally involved.[6] The observed efficacy of plasma exchange for treating WEBINO syndrome suggests that humoral factors, such as anti-AQP4 antibody, contributed to its development in this patient. Hence, because not only MS but also anti-AQP4 antibody-positive NMO patients can present with WEBINO syndrome, diagnosis of NMO should not be excluded in patients with WEBINO syndrome, or even bilateral MLF syndrome.

Funding

This research received no specific grant from any funding agency in the public, commercial, or not-for-profit sectors.

Conflict of interest statement

The authors report no conflicts of interest.

References

1. McGettrick P and Eustace P. The w.e.h.i.n.o. syndrome. *Neuro-ophthalmol* 1985; 5: 109–115.
2. Strominger MB, Mincy EJ, Strominger AI and Strominger NL. Bilateral internuclear ophthalmoplegia with absence of convergent eye movements. Clinicopathologic correlation. *J Clin Neuroophthalmol* 1986; 6: 57–65.
3. Ushio M, Iwasaki S, Chihara Y and Murofushi T. Wall-eyed bilateral internuclear ophthalmoplegia in a patient with progressive supranuclear palsy. *J Neuroophthalmol* 2008; 28: 93–96.
4. Lennon VA, Wingerchuk DM, Kryzer TJ, et al. A serum autoantibody marker of neuromyelitis optica: distinction from multiple sclerosis. *Lancet* 2004; 364: 2106–2112.
5. Lennon VA, Kryzer TJ, Pittock SJ, Verkman AS and Hinson SR. IgG marker of optic-spinal multiple sclerosis binds to the aquaporin-4 water channel. *J Exp Med* 2005; 202: 473–477.
6. Matsushita T, Isobe N, Matsuoka T, et al. Aquaporin-4 autoimmune syndrome and anti-aquaporin-4 antibody-negative opticospinal multiple sclerosis in Japanese. *Mult Scler* 2009; 15: 834–847.
7. Wingerchuk DM, Lennon VA, Pittock SJ, Lucchinetti CF and Weinshenker BG. Revised diagnostic criteria for neuromyelitis optica. *Neurology* 2006; 66: 1485–1489.
8. Pittock SJ, Lennon VA, Krecke K, Wingerchuk DM, Lucchinetti CF and Weinshenker BG. Brain abnormalities in neuromyelitis optica. *Arch Neurol* 2006; 63: 390–396.
9. Wingerchuk DM, Lennon VA, Lucchinetti CF, Pittock SJ and Weinshenker BG. The spectrum of neuromyelitis optica. *Lancet Neurol* 2007; 6: 805–815.
10. Chen C-M and Lin S-H. Wall-eyed bilateral internuclear ophthalmoplegia from lesions at different levels in the brainstem. *J Neuroophthalmol* 2007; 27: 9–15.

Brain Pathology ISSN 1015-6305

RESEARCH ARTICLE

Reappraisal of Aquaporin-4 Astrocytopathy in Asian Neuromyelitis Optica and Multiple Sclerosis Patients

Takeshi Matsuoka[1,2]; Satoshi O. Suzuki[2]; Toshihiko Suenaga[3]; Toru Iwaki[2]; Jun-ichi Kira[1]

[1] Departments of Neurology and [2] Neuropathology, Neurological Institute, Graduate School of Medical Sciences, Kyushu University, Fukuoka, Japan.
[3] Department of Neurology, Tenri Hospital, Tenri, Japan.

Keywords
antibody, aquaporin-4, astrocyte, multiple sclerosis, neuromyelitis optica.

Corresponding author:
Satoshi O. Suzuki, MD, PhD, Department of Neuropathology, Neurological Institute, Graduate School of Medical Sciences, Kyushu University, 3-1-1 Maidashi, Higashi-ku, Fukuoka 812-8582, Japan (E-mail: *sosuzuki@np.med.kyushu-u.ac.jp*)

Received 11 August 2010; accepted 9 December 2010.

doi:10.1111/j.1750-3639.2011.00475.x

Abstract

Selective aquaporin-4 (AQP4) loss and vasculocentric complement and immunoglobulin deposition are characteristic of neuromyelitis optica (NMO). We recently reported extensive AQP4 loss in demyelinated and myelinated layers of Baló's lesions without perivascular immunoglobulin and complement deposition. We aimed to reappraise AQP4 expression patterns in NMO and multiple sclerosis (MS). We evaluated AQP4 expression relative to glial fibrillary acidic protein, extent of demyelination, lesion staging (CD68 staining for macrophages), and perivascular deposition of complement and immunoglobulin in 11 cases with NMO and NMO spectrum disorders (NMOSD), five with MS and 30 with other neurological diseases. The lesions were classified as actively demyelinating (n = 66), chronic active (n = 86), chronic inactive (n = 48) and unclassified (n = 12). Six NMO/NMOSD and two MS cases showed preferential AQP4 loss beyond the demyelinated areas, irrespective of lesion staging. Five NMO and three MS cases showed AQP4 preservation even in actively demyelinating lesions, despite grave tissue destruction. Vasculocentric deposition of complement and immunoglobulin was detected only in NMO/NMOSD patients, with less than 30% of actively demyelinating lesions showing AQP4 loss. Our present and previous findings suggest that antibody-independent AQP4 loss can occur in heterogeneous demyelinating conditions, including NMO, Baló's disease and MS.

Abbreviations: ALS = amyotrophic lateral sclerosis; AQP4 = aquaporin-4; BBB = blood-brain barrier; BCS = Baló's concentric sclerosis; CNS = central nervous system; GFAP = glial fibrillary acidic protein; H & E = hematoxylin and eosin, IgG = immunoglobulin G; KB = Klüver-Barrera; LESCL = longitudinally extensive spinal cord lesion; MG = myasthenia gravis; MS = multiple sclerosis; MRI = magnetic resonance imaging; NMO = neuromyelitis optica; NMOSD = neuromyelitis optica spectrum disorder; OSMS = opticospinal multiple sclerosis; SCD = spinocerebellar degeneration; SPG = spastic paraplegia.

INTRODUCTION

Multiple sclerosis (MS) and neuromyelitis optica (NMO) are inflammatory demyelinating diseases of the central nervous system (CNS). The pathological hallmark in MS is sharply demarcated demyelinating plaques with axons relatively preserved, suggesting autoimmune attacks targeting CNS myelin. By contrast, NMO shows selective and severe attacks on both axons and myelin of the optic nerves and spinal cord, resulting in necrotic cavitation. In this condition, longitudinally extensive spinal cord lesions (LESCLs) extending over three vertebral segments are characteristic on magnetic resonance imaging (MRI) (54).

Although the nosological position of NMO has long been a matter of debate, the recent discovery of a specific IgG against NMO, designated NMO-IgG (28), suggests that NMO is distinct from MS and has a fundamentally different etiology. This IgG targets the aquaporin-4 (AQP4) water channel protein (29), which is strongly expressed on astrocyte foot processes at the blood–brain barrier (BBB) (18). Autopsied NMO cases show a loss of AQP4 immunostaining in inflammatory lesions (38, 45). The vasculocentric deposition of complement and immunoglobulins in NMO lesions (30) suggests a humoral immune attack against AQP4 on astrocytes, especially as the NMO-IgG/anti-AQP4 antibody is cytotoxic to astrocytes *in vitro* and *in vivo* in the presence of complement (3, 5, 19–21, 46, 47, 52).

However, the predictive value of the NMO-IgG/anti-AQP4 antibody is only moderate; 30%–73% in Caucasians (9, 10, 17, 28, 42), 63% in northern Japanese with opticospinal MS (OSMS) (39), 27% in southern Japanese with OSMS (31) and 33% in Caribbean people (6). On the other hand, 5%–15% of MS cases are positive

for NMO-IgG or anti-AQP4 antibody. Pittock *et al* (43) described that 10% of NMO-IgG-positive patients had brain lesions that were indistinguishable from those in MS patients, whereas some patients also showed extensive brain lesions (34, 36, 43). By contrast, LESCLs are seen in about a quarter of classical Asian MS patients (8, 32, 37, 49), compared with 12.5% of Caucasian MS patients (4). Asian patients with MS show necrotizing lesions with occasional cavity formation in the spinal cord, optic nerve and cerebrum (12, 14, 40, 50), reflecting severe inflammation. These findings suggest considerable overlap between NMO and MS, especially in Asians.

In addition, Baló's concentric sclerosis (BCS), a rare variant of MS with huge brain lesions showing concentric rings of alternating demyelination and normal myelin layers, is more common in Asians, such as Filipinos (25), southern Han Chinese (53) and Taiwanese (7), than in other races. Asian MS patients can also show concentric demyelinating lesions in the spinal cord and the optic chiasm pathologically (16), representing an intermediate between BCS and MS. We recently reported extensive AQP4 loss in both demyelinated and myelinated layers of BCS lesions in the absence of perivascular immunoglobulin and complement deposition (33). Interestingly, development of BCS-like lesions in the brainstem on MRI was recently reported in Asian patients with not only classical MS (23) but also NMO (11). Other than two pivotal neuropathological studies (38, 45), only a few case reports have examined AQP4 expression in NMOs with varying results (13, 24, 51, 57). Furthermore, although AQP4 expression in MS has also been examined in some studies (38, 45, 48), there are inconsistencies among their conclusions. We therefore decided to perform a systematic immunohistological reappraisal of AQP4 expression relative to astrocyte marker expression, the extent of demyelination, lesion staging and the perivascular deposition of complement and immunoglobulin in Asian NMO and MS patients to clarify the contribution of astrocyte damage, including AQP4 loss to the lesion formation, in these conditions.

MATERIALS AND METHODS

Autopsy tissue and patient characterization

The study was performed on archival autopsied brain, optic nerve and spinal cord materials from 10 NMO cases, including one anti-AQP4 antibody-positive case, one case with NMO spectrum disorder (NMOSD), and five cases with MS. All but the anti-AQP4 antibody-positive case from Tenri Hospital were from the Department of Neuropathology, Kyushu University. NMO/NMOSD diagnosis was based on the Wingerchuk criteria (54–56), while MS was diagnosed according to the Poser criteria (44). The clinical findings are summarized in Table 1. The median age at autopsy was 44.0 years old (range 28–88) in the NMO/NMOSD cases (nine females and two males) and 39.0 years old (range 12–52) in the MS cases (three females and two males). Disease durations ranged from 0.4 to 17.0 years in the NMO/NMOSD group (median, 4.7 years), and from 0.7 to 21.0 years in the MS group (median, 3.1 years). In addition, we used the same set of control cases with other neurological diseases as in our previous study (33): myasthenia gravis (MG) (n = 2), spastic paraplegia type 2 (n = 1), amyotrophic lateral sclerosis (n = 6), hippocampal sclerosis with temporal lobe epilepsy (n = 5), muscular dystrophy (n = 1), encephalitis (n = 3), including one with anti-N-methyl-D-aspartate receptor antibody and another with anti-thyroglobulin antibody, spinocerebellar degeneration (n = 1),

Table 1. Summary of clinical and pathological findings of Japanese patients with neuromyelitis optica and multiple sclerosis. Abbreviations: MS = multiple sclerosis; N.A. = not applicable; NMO = neuromyelitis optica (Wingerchuk *et al* (55, 56)); NMOSD = neuromyelitis optica spectrum disorders (Wingerchuk *et al* (57)).

Autopsy	Age (years)	Sex	Disease duration (years)	Relapse rate	Clinically estimated sites of lesions	Pathologically determined sites of lesions
NMO-1	44	F	3.8	1.6	O2, S6	O, S, Bs, Cr, Cl
NMO-2	44	F	1.8	2.8	O2, Bs3, S2	O, S, Bs, Cr
NMO-3	48	F	0.5	4.0	O2, Bs1, S1	O, S, Bs, Cr
NMO-4	32	M	6.3	1.1	O1, Bs2, S7	O, S, Bs, Cl, Cr
NMO-5	28	F	4.7	0.6	O3, Bs2, S2	O, S, Bs, Cl, Cr
NMO-6	35	F	7.0	1.4	O4, Bs4, S4	O, S, Bs, Cr
NMO-7	37	F	10.8	1.5	O9, Bs2, S14	O, S, Bs, Cl, Cr
NMO-8	47	F	8.3	0.1	O2, Bs1, S2	O, S, Bs, Cr
NMO-9	54	F	4.0	1.3	O1, S6	O, S
NMO-10*	37	F	17.0	1.1	O8, Bs1, S9, Cr3	Bs, S, Cr
NMOSD	88	M	0.4	0.0	S1	O, S
MS-1	12	F	5.0	2.2	O6, Bs1, S2, Cr3	O, Bs, S, Cr, Cl
MS-2	35	M	3.1	1.0	O1, Bs2, S2, Cr2	O, Bs, S, Cr
MS-3	52	F	1.3	1.5	Bs1, Cr3	Bs, Cr
MS-4	45	F	0.7	1.4	Bs2, S2	O, S, Bs
MS-5	39	M	21.0	0.5	O1, Bsx, Clx, Crx	O, Bs, Cl, Cr

Lesion sites in clinical exacerbations: O = optic nerve; S = spinal cord; Bs = brainstem; Cl = cerebellum; Cr = cerebrum. Numbers indicate exacerbations in each lesion site (eg, O2 represents two episodes of optic neuritis). Asterisk indicates a NMO case with known anti-AQP4 antibody seropositivity.

Table 2. Antibodies used for immunohistochemistry. Abbreviations: AQP4 = aquaporin-4, GFAP = glial fibrillary acidic protein; N.D. = not done.

Antibody	Type	Dilution	Antigen retrieval	Source
Aquaporin-4				
AQP4	rabbit polyclonal	1:500	N.D.	Santa Cruz Biotechnology, California, USA
Complement				
C3d	rabbit polyclonal	1:1000	Autoclave/10 mM citrate buffer	DakoCytomation, Glostrup, Denmark
C9neo	mouse monoclonal	1:1000	Autoclave/10 mM citrate buffer	Abcam plc, Cambridge, UK
Macrophage/microglia				
CD68	mouse monoclonal	1:200	Autoclave/10 mM citrate buffer	DakoCytomation, Glostrup, Denmark
Astrocyte				
GFAP	rabbit polyclonal	1:1000	N.D.	DakoCytomation, Glostrup, Denmark
Immunoglobulin				
IgG	rabbit polyclonal	1:10 000	Autoclave/10 mM citrate buffer	DakoCytomation, Glostrup, Denmark
IgM	rabbit polyclonal	1:10 000	Autoclave/10 mM citrate buffer	DakoCytomation, Glostrup, Denmark
Lymphocyte				
CD45RO	mouse monoclonal	1:200	Autoclave/10 mM citrate buffer	DakoCytomation, Glostrup, Denmark
CD20	mouse monoclonal	1:200	Autoclave/10 mM citrate buffer	DakoCytomation, Glostrup, Denmark

vasculitis (n = 3), cerebral infarction (n = 1), Pick's disease (n = 1), progressive supranuclear palsy (n = 3) and multiple system atrophy (n = 3).

Tissue preparation and immunohistochemistry

Autopsied specimens were fixed in 10% formalin and processed into paraffin sections. Sections were routinely stained with hematoxylin and eosin (H & E), Klüver-Barrera (KB), and Bodian or Bielschowsky silver impregnation. Primary antibodies for immunohistochemistry are listed in Table 2. All sections were deparaffinized in xylene and rehydrated in an ethanol gradient. Endogenous peroxidase activity was blocked with 0.3% H_2O_2/methanol. The sections were then incubated with primary antibody at 4°C overnight. After rinsing, the sections were subjected to either a streptavidin-biotin complex method or an enhanced indirect immunoperoxidase method using Envision (DakoCytomation, Glostrup, Denmark). Immunoreactivity was detected using 3,3′-diaminobenzidine and sections were counterstained with hematoxylin. Immunohistochemistry for activated complement, immunoglobulins, T cell and B cell markers was performed in randomly selected lesions.

Staging of demyelinating lesions

We classified demyelinating lesions into the following three stages: actively demyelinating lesions, chronic active lesions and chronic inactive lesions based on the density of infiltrating macrophages (26). Briefly, actively demyelinating lesions had active destructive lesions densely and diffusely infiltrated with macrophages phagocytosing myelin debris, as identified by Luxol fast blue staining. Chronic active lesions were those showing hypercellularity of macrophages restricted to the periphery of the lesions. Chronic inactive lesions were those showing no increase in macrophages throughout the lesions.

According to the staging protocol, NMO lesions (n = 149) were classified as 42 actively demyelinating lesions, 72 chronic active lesions and 35 chronic inactive lesions, whereas MS lesions (n = 51) were classified into 24 actively demyelinating lesions, 14 chronic active lesions and 13 chronic inactive lesions. In addition, we noted 12 lesions in NMO (seven lesions) and MS cases (five lesions) that did not meet the staging criteria. All of these lesions had perivascular deposition of both activated complement and immunoglobulins, but no macrophage infiltration, and lacked any myelin or AQP4 loss. These lesions were thus analyzed separately.

Figure 1. Loss of AQP4 expression in active lesions of NMO. **(A–F)** Serial sections of an actively demyelinating cerebral lesion from NMO-10 with known anti-AQP4 antibody seropositivity representing Pattern A. Arrowheads indicate the same blood vessel. **A.** Sharply demarcated demyelinating plaque is noted in the cerebral white matter. **B.** GFAP immunopositivity is decreased in the lesion. **C.** AQP4 immunopositivity is lost beyond the area with myelin/GFAP loss. **D.** Numerous macrophages contain myelin debris (arrowheads). **E.** Degeneration of vascular foot processes is evident by GFAP immunostaining. **F.** AQP4 immunoreactivity is absent even in the degenerated astrocytes. **(G–O)** Serial sections of corpus callosum lesions from NMO-4 representing Patterns A & N. **G.** The corpus callosum demonstrates severe demyelination with tissue necrosis (dagger). **H.** CD68-positive macrophages diffusely infiltrate the lesions. **I.** GFAP immunostaining shows numerous reactive astrocytes in the surrounding region, but it decreases in the necrotic lesion center and focal perivascular areas with positive myelin staining (arrowhead in G and I). **J.** AQP4 immunostaining reveals a pattern similar to that of GFAP staining, but decreases more extensively in the still-myelinated area indicated by the asterisk in G. **K.** High magnification of the necrotic area indicated by the dagger in G. Numerous foamy macrophages containing myelin debris are present. (L–O) High magnification of the still-myelinated area indicated by the asterisk in G. **L.** Still-preserved myelin with some foamy macrophages without myelin debris. **M.** CD68-immunopositive foamy macrophages are present among the preserved myelin. **N.** GFAP immunostaining reveals degenerated astrocytes and astrocytic vascular foot processes. **O.** AQP4 immunoreactivity is completely lost despite the presence of astrocytes. **A, D, G, K, L, KB; B, E, I, N**, GFAP immunohistochemistry (IHC); **C, F, J, O**, AQP4 IHC; H, M, CD68 IHC. Scale bar = 1 mm **(A–C)**; 300 μm **(G–J)**; 50 μm **(E, F, L–O)**; 20 μm **(D, K)**. AQP4 = aquaporin-4; GFAP = glial fibrillary acidic protein; KB = Klüver-Barrera staining; NMO = neuromyelitis optica.

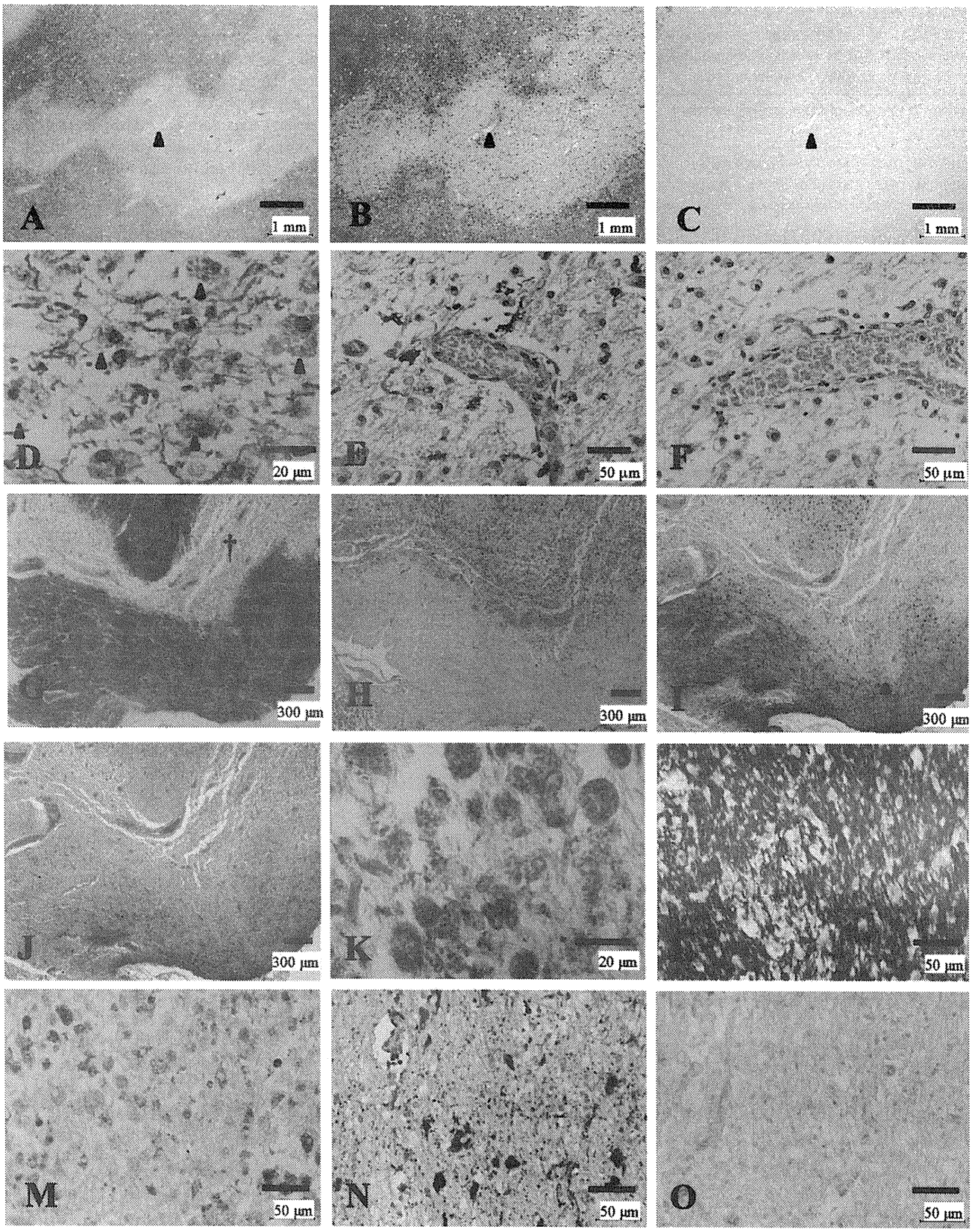

Table 3. Classification of demyelinating lesions according to aquaporin-4 and glial fibrillary acid protein immunostaining and Klüver-Barrera staining. Abbreviations: AQP4 = aquaporin-4; GFAP = glial fibrillary acidic protein; KB = Klüver-Barrera staining.

Lesion pattern	Extents of AQP4 and myelin loss	GFAP expression
Pattern A	AQP4 loss or decrease > myelin loss	(+)
Pattern B	AQP4 loss or decrease = myelin loss	(+)
Pattern C	AQP4 loss or decrease < myelin loss	(+)
Pattern D	AQP4 totally preserved in areas of myelin loss	(+)
Pattern N	necrosis or cavity formation	(–)

Comparison of AQP4 expression with myelin loss and astrogliosis

For each lesion, we compared the level of AQP4 expression with the degree of myelin loss and the level of glial fibrillary acidic protein (GFAP) expression. AQP4 expression levels in region-matched unaffected areas (ie, gray matter or white matter) in the same section were used as an internal control. When the presence of astrocytes was not confirmed by GFAP immunostaining caused by total replacement of a lesion with foamy macrophages, or when cavity formation was evident, the lesion was classified as a destructive necrotic lesion. Accordingly, 15 lesions with severe necrosis or cavity formation (nine in NMO patients and six in MS patients) were determined.

Using serial sections of demyelinating lesions, we divided the expression patterns of AQP4 immunoreactivity relative to the intensity of GFAP immunoreactivity and myelin (KB) staining into the following five patterns (Table 3): Pattern A (area of diminished AQP4 immunoreactivity extending over that of myelin loss), Pattern B (area of diminished AQP4 immunoreactivity conforming with that of myelin loss), Pattern C (area of diminished AQP4 immunoreactivity less than that of myelin loss), Pattern D (preserved AQP4 immunoreactivity with loss of myelin staining) and Pattern N (necrosis or cavity formation; GFAP-negative,

Table 4. Summary of aquaporin-4 immunoreactivity patterns in demyelinating lesions in cases with neuromyelitis optica (NMO) or NMO spectrum disorders. Abbreviations: AQP4 = aquaporin-4; NMO = neuromyelitis optica; NMOSD = neuromyelitis optica spectrum disorder; N.A. = specimen not available.

Autopsy	Stage	Cerebrum	Brainstem	Cerebellum	Spinal cord	Optic nerve
Preferential AQP4 loss or decrease						
NMO-2	Active	A (1)	A&N (1)	N.A.	B&N (1)	N.A.
	Chronic active	B&N (1), C&N (1)			A&N (3), B&N (1)	
	Chronic inactive	C (2)			C&N (1)	
NMO-3	Active	B&N (1)				A&N (1)
	Chronic active	B&N (1), C&N (1)	A (1)		A&N (3)	A&N (1)
	Chronic inactive	C&N (3)				
NMO-4	Active	A (1), A&N (3), B (1), B&N (1)	A&N (2), B&N (1)	B (2)	B&N (1)	D (1)
	Chronic active	B&N (1)	B (2)		A&N (1), B&N (1), C&N (1)	
	Chronic inactive	D (1)				
NMO-7	Active		A (3), B (1)		A&N (2)	
	Chronic active	C (3)	A (3), B (1), C (1), C&N (1)			
	Chronic inactive	C (1), D (2)	C&N (2)			D&N (1)
NMO-10	Active	A (1), A&N (1), N (1)				N.A.
	Chronic active	B (2), B&N (1), C&N (1)	C&N (1)		A&N (1), C&N (1)	
	Chronic inactive	D (1), N (1)				
NMOSD	Active				A&N (1), B&N (1), N (1)	
	Chronic active				B&N (1)	
	Chronic inactive					D (1)
Preserved AQP4 expression						
NMO-1	Active	D&N (1)	N (2)			
	Chronic active		D (1)		D (1)	D (1)
	Chronic inactive	D&N (1)				
NMO-5	Active	D&N (1), D (3)				
	Chronic active	D (5), D&N (4)	D&N (1), D (2)	D (2)		
	Chronic inactive	D (3)	D&N (1)		D&N (1)	D (1)
NMO-6	Active	D (1)				
	Chronic active	D (5), D&N (2)	D&N (1)	D (1)		
	Chronic inactive	D (1)	D&N (1)		D (1), D&N (1)	D&N (1)
NMO-8	Chronic active	D (1), D&N (5)	D&N (1)		D&N (1)	D (1)
	Chronic inactive	D (1), D&N (1)	D (2), N (1)			N (1)
NMO-9	Active				D&N (1), N (2)	D (1)
	Chronic active				D&N (1)	

Blank cell = No lesions.

AQP4-negative and myelin-negative by definition). Patterns associated with focal necrosis or cavity formation were expressed as "Patterns X & N" (X = A, B, C or D).

RESULTS

Immunohistochemical findings in control brains

AQP4 and GFAP staining patterns as well as the deposition of immunoglobulins and activated complement in normal and diseased CNS tissues were described in detail in our previous report (33). Briefly, in normal cerebral tissues, AQP4 staining was more pronounced in the cortex than in the white matter, with staining emphasized in the perivascular foot processes. The glial limiting membranes and subependymal astrocytes also strongly expressed AQP4. By contrast, GFAP immunoreactivity was preferentially observed in the cerebral white matter while in the cortex, and except for the strong staining of the glial limiting membranes, only a few astrocytes were immunopositive for GFAP. Reactive astrocytes and gliotic scars were strongly immunopositive for both AQP4 and GFAP. In control cases, faint, diffuse IgG immunoreactivity in the neuronal soma, neuropil, oligodendrocytes, astrocytes, glial limiting membranes and ependymal epithelium was observed, but not in the white matter. IgM, C3d and C9neo immunoreactivities were generally confined to a small number of blood vessel walls and the perivascular regions, if any. Activated complement was not usually co-localized with immunoglobulins.

Immunohistochemical findings in NMO and NMO spectrum disorders

Preferential loss or decrease of AQP4 immunoreactivity in actively demyelinating lesions and upregulation of AQP4 in chronic inactive lesions in NMO/NMOSD cases

Five NMO cases (NMO-2, 3, 4, 7 and 10) and an NMOSD case showed preferential loss of AQP4 in at least one of the actively demyelinating lesions beyond the demyelinated areas (Pattern A) (Figure 1, Table 4). NMO-10, with known anti-AQP4 antibody seropositivity, showed extensive AQP4 loss, not only in the lesion center where numerous myelin-laden foamy macrophages had infiltrated (Figure 1D), but also in the surrounding, GFAP-immunopositive myelinated areas (Figure 1A–C). In actively demyelinating lesions, GFAP immunostaining revealed highly degenerated astrocytic vascular foot processes (Figure 1E), and AQP4 expression was totally lost in these GFAP-immunopositive structures (Figure 1F).

In addition to the actively demyelinating lesions and necrotic lesions (Figure 1G, dagger, Figure 1K), still-myelinated areas at the lesion periphery occasionally showed a remarkable decrease in both GFAP and AQP4 expression in Pattern A, which was considered to represent early lesions (Figure 1G–O, asterisk in G). In such lesions, GFAP immunostaining revealed remaining highly degenerated astrocytes and their vascular foot processes (Figure 1N). Despite the existence of remnant astrocytes, AQP4 immunoreactivity was hardly detectable in such lesions (Figure 1O).

In contrast to the loss of both GFAP and AQP4 expression in acute lesions in this group, all the chronic inactive lesions in the NMO/NMOSD cases, including those in the anti-AQP4 antibody-seropositive case (NMO-10; Figure 2A–D), showed upregulation of AQP4 in areas with various degrees of reparative gliosis (either Pattern C or D) (Figure 2, Table 4).

Preserved AQP4 expression in actively demyelinating lesions in NMO cases

While the above-mentioned cases showed typical AQP4 and GFAP loss in active demyelinating lesions as reported previously (38, 45), five cases (NMO-1, 5, 6, 8 and 9) showed no preferential loss of AQP4 (Pattern D) in any lesions, including actively demyelinating lesions except for necrotic or cavitary lesions where no astrocytes were present (Pattern N) (Figure 3D–F, Table 4).

Heterogeneous AQP4 expression in actively demyelinating lesions

Among the NMO cases with preferential loss of AQP4 (Pattern A or B) in active lesions, we found a subset of cases showing lesion-to-lesion heterogeneity in AQP4 expression pattern, even among the active lesions (Figure 3G–L; compare with Figure 1G–O, Table 4). These included three NMO cases (NMO-4, 7 and 10) and one NMOSD case. Pattern D was observed in an active lesion in one case (NMO-4), and Pattern C was observed in chronic active lesions in five cases (NMO-2, 3, 4, 7 and 10) (Table 4). The NMO-4 case had repeated attacks of transverse myelitis and acutely developed a single episode of bilateral optic neuritis 1 month prior to death. As described earlier, the corpus callosum contained partially necrotized actively demyelinating lesions, with diminished AQP4 immunoreactivity extending over the loss of myelin staining and areas with reactive astrocytes, representing Patterns A and N (Figure 1G–O). Approximately half of the actively demyelinating lesions in this case were classified as Pattern A (Table 4). By contrast, the optic chiasm had actively demyelinating lesions densely infiltrated with macrophages containing myelin debris (Figure 3G–I), where both GFAP and AQP4 was expressed diffusely in the demyelinated lesions and the surrounding normal-looking areas (Figure 3J, K). At higher magnification, the demyelinating lesions were diffusely stained for AQP4 (Figure 3L) in many hypertrophic astrocytes and their processes, being classified as Pattern D.

Immunohistochemical findings in MS

Three MS cases (MS-1, 2 and 5) showed preservation of AQP4 in actively demyelinating lesions, whereas the other two (MS-3 and 4) showed preferential AQP4 loss in active lesions of both acute and chronic stages (Pattern A or B) (Table 5). All the MS cases showed AQP4 immunoreactivity in gliotic areas of chronic inactive lesions, if present (Pattern C or D) (Table 5).

Preferential decrease of AQP4 staining in actively demyelinating lesions

The MS-3 case had cerebral signs at disease onset and brainstem signs at relapse, but neither optic neuritis nor myelitis was noted.

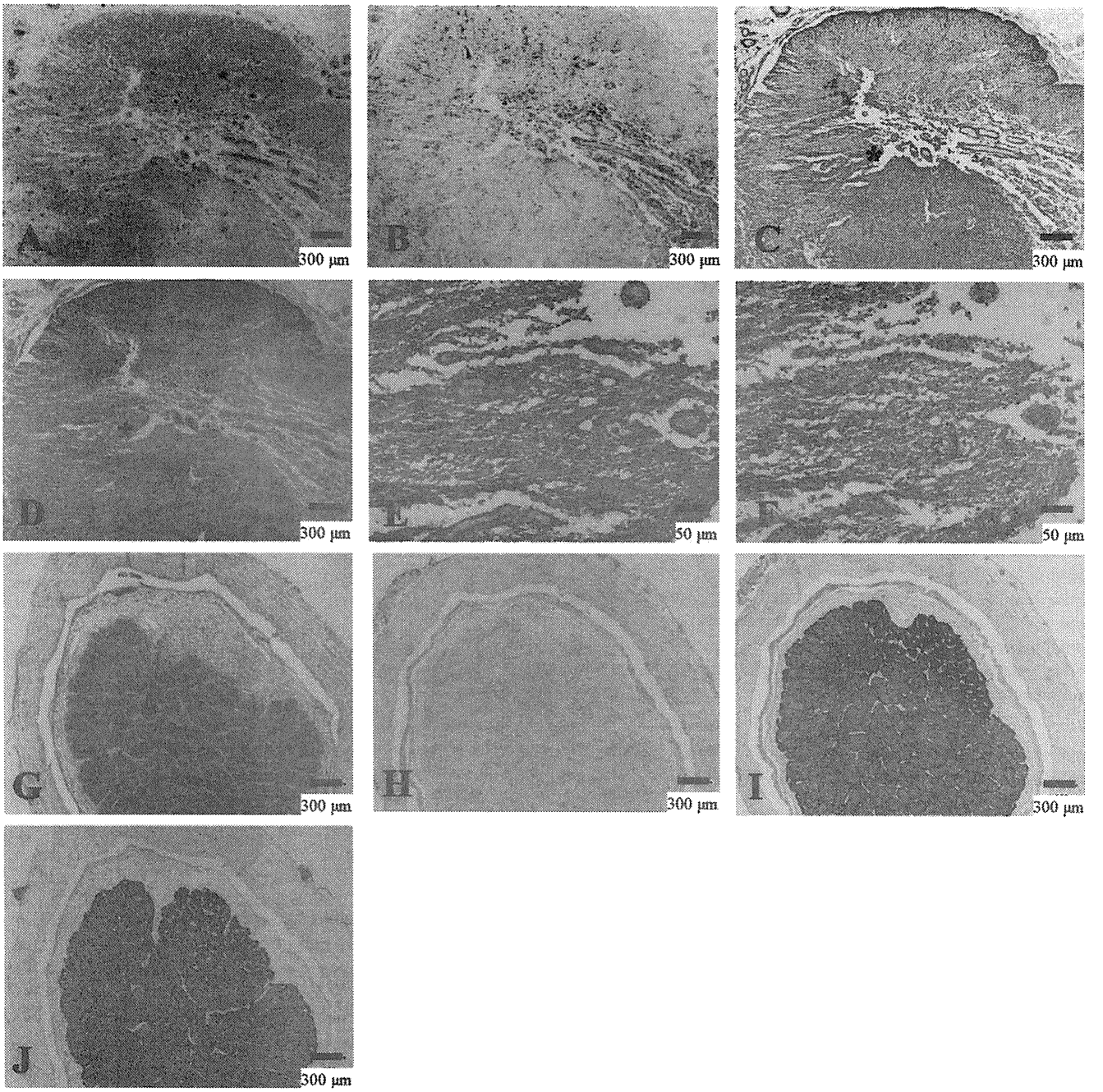

Figure 2. Upregulation of AQP4 in chronic NMO lesions. (**A–F**) Serial sections of chronic active demyelinating lesions in the spinal cord of NMO-10 representing Pattern C and N. **A.** The spinal cord has irregularly-shaped demyelinating lesions with necrosis and cavity formation. Reactive proliferation of capillary vessels is noted. **B.** CD68-positive macrophages are still abundant in the perivascular regions. **C.** The lesion is immunopositive for GFAP except for in the cavity center. **D.** Upregulation of AQP4 in extensively demyelinated lesions. **E.** High magnification in the lesion indicated by the asterisk in C shows increased GFAP immunoreactivity. **F.** The same area as E demonstrates AQP4 staining in areas of astrogliosis. (**G–J**) Serial sections of chronic inactive demyelinating lesions in the optic nerve from NMOSD, representing Pattern D. **G.** Sharply demarcated demyelinating plaque in the optic nerve. **H.** Macrophage infiltration is absent. **I.** GFAP-positive chronic astrogliosis covers the demyelinating plaque. **J.** AQP4 expression is upregulated in the areas of chronic astrogliosis. **A, G**, KB staining; **B, H**, CD68 immunohistochemistry (IHC); **C, E, I**, GFAP IHC; **D, F, J**, AQP4 IHC. Scale bar = 300 μm (**A–D, G–J**); 50 μm (**E, F**). AQP4 = aquaporin-4; GFAP = glial fibrillary acidic protein; KB = Klüver-Barrera staining; NMO = neuromyelitis optica; NMOSD = NMO spectrum disorder.

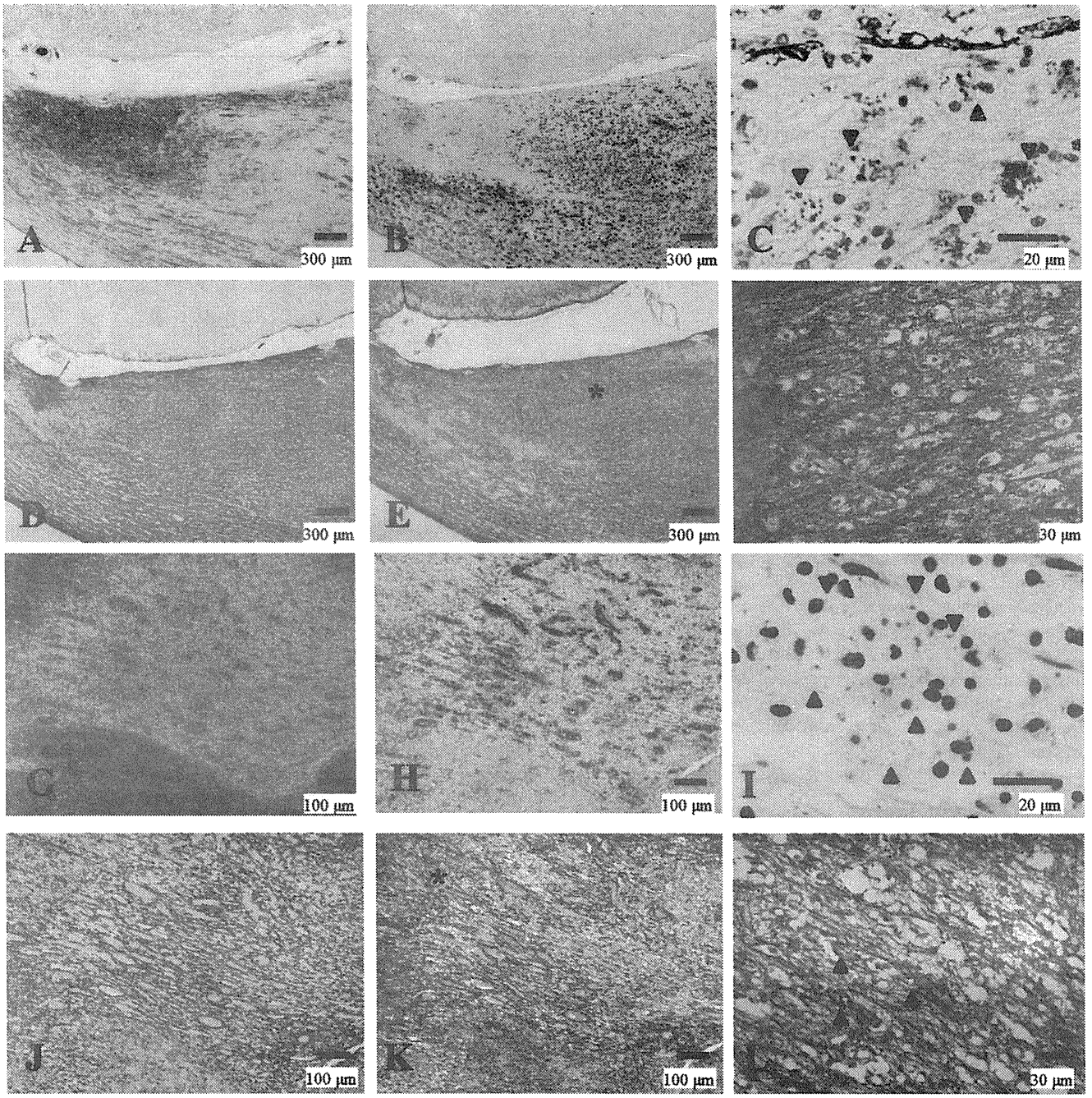

Figure 3. Preserved AQP4 immunoreactivity in actively demyelinating NMO lesions. (**A–F**) Serial sections of an actively demyelinating lesion from NMO-6 representing Pattern D. **A.** Demyelinating plaque in the corpus callosum. **B.** The lesion is infiltrated by numerous foamy macrophages stained with CD68. **C.** Macrophages containing myelin debris (arrowheads). **D.** The lesion shows strong GFAP immunoreactivity. **E.** The same area as in **D**, with AQP4 expression as strong and diffuse as that of GFAP. **F.** High magnification of the area indicated by the asterisk in **E.** AQP4 expression is preserved despite dense macrophage infiltration. (**G–L**) Serial sections of an optic nerve lesion from NMO-4 representing Pattern D. **G.** Sharply demarcated demyelinating plaques are seen. **H.** The optic chiasm is densely infiltrated with foamy macrophages. **I.** Numerous macrophages contain myelin debris. **J.** Numerous GFAP-positive reactive astrocytes in the lesion center and the surrounding areas. **K.** AQP4 immunoreactivity is enhanced at the lesion center. **L.** High magnification of the area indicated by the asterisk in **K** demonstrates AQP4 staining along the entire processes and outlining the cytoplasm of hypertrophic reactive astrocytes (arrowheads). **A, C, G, I**, KB staining; **B, H**, CD68 immunohistochemistry (IHC); **D, J**, GFAP IHC; **E, F, K, L**, AQP4 IHC. Scale bar = 300 μm (**A, B, D, E**); 100 μm (**G, H, J, K**);30 μm (**F, L**); 20 μm (**C, I**). AQP4 = aquaporin-4; GFAP = glial fibrillary acidic protein; KB = Klüver-Barrera staining; NMO = neuromyelitis optica.

Table 5. Summary of aquaporin-4 immunoreactivity patterns in demyelinating lesions in cases with multiple sclerosis. Abbreviations: AQP4 = aquaporin-4; MS = multiple sclerosis.

Autopsy	Stage	Cerebrum	Brainstem	Cerebellum	Spinal cord	Optic nerve
Preferential AQP4 loss or decrease						
MS-3	Active	A&N (1), B (3), B&N (1), N (1)	A&N (2), N (2)			
	Chronic active	B (2)				
	Chronic inactive	C (1)				
MS-4	Active		A (1), B (3)			
	Chronic active		B (1)		A &N (3), A (1)	C (1)
Preserved AQP4 expression						
MS-1	Active		N (3)			
	Chronic active	D&N (1)				
	Chronic inactive				D (1), D&N (2)	
MS-2	Active		D (1), D&N (1)			D (1)
	Chronic active		D (2)			D (1)
MS-5	Active	D (2)	D (1)	D (1)		
	Chronic active	D (1)	D (1)			
	Chronic inactive	D (4), D&N (3)		D (1)		D (1)

Blank cell = no lesions.

Notably, AQP4 loss was observed in both the centers of actively demyelinating plaques with dense perivascular lymphocytic cuffing in the cerebral peduncle, and in the periphery of the lesions where KB staining indicated preserved myelin with diffuse macrophage infiltration. This lesion was thus classified as Pattern A (see asterisks in Figure 4A–D). At higher magnification, GFAP immunostaining revealed degeneration of astrocytes and disruption of the perivascular glia limitants (Figure 4E). AQP4 expression was almost totally lost even in the scattered GFAP-positive structures (Figure 4F).

Loss of AQP4 expression in BCS-like concentric spinal cord lesions in an MS case

MS-4 had concentric lesions showing alternating rings with and without myelin in the chronic active stage, accompanied by perivascular macrophage infiltration in the spinal cord (Figure 4G, H). AQP4 loss was seen not only in the sharply demyelinated layers but also in the preserved myelin layers, and this lesion was classified as Pattern A (Figure 4I, J). High magnification demonstrated that AQP4 expression was lost on the astrocytic processes and reactive astrocytes, even though they were positive for GFAP (Figure 4K, L).

The actively demyelinating lesions in these two cases were classified as Pattern A or B (loss of AQP4).

Relationship between complement and immunoglobulin deposition and AQP4 loss

In the actively demyelinating lesions of the NMO/NMOSD cases, depositions of activated complement and immunoglobulins in the perivascular areas were observed in 28.6% of Pattern A lesions (Figures 5A–H and 7A). In chronic active lesions, such depositions were noted in 10%–15% of Patterns A, B and C. In chronic inactive lesions, one of 17 (6%) Pattern D lesions had perivascular deposits. However, MS cases did not have depositions in any demyelinated lesion (Figure 5I, J).

Four of the six cases with NMO/NMOSD that had AQP4 loss (Pattern A) showed concurrent perivascular deposition of activated complement and immunoglobulins in at least one actively

Figure 4. Preferential loss of AQP4 immunoreactivity in MS. (**A–F**) Serial sections of actively demyelinating lesions in the midbrain of MS-3 without optic-spinal lesions representing Patterns A & N. **A.** A demyelinating plaque in the acute stage in the cerebral peduncle, with dense perivascular lymphocytic cuffing. Myelin is still preserved at the periphery of the lesion (asterisk) despite CD68-positive foamy macrophage infiltration (**B**). **C.** GFAP immunoreactivity is decreased in the lesion center while numerous reactive astrocytes are present at the lesion edge and surrounding areas (asterisk). **D.** AQP4 immunoreactivity is extensively lost in not only the demyelinating center but also in the surrounding areas, where GFAP immunoreactivity is preserved (asterisk). **E.** High magnification of the area indicated by an arrowhead in C and D. Vascular foot processes are destroyed but there are remaining GFAP-positive astrocytes. **F.** The same microscopic field as in **E.** Astrocytes are devoid of AQP4 immunoreactivity. (**G–L**) Serial sections of chronic active Baló-like concentric lesions in the spinal cord from MS-4 representing Pattern A. **G.** The spinal cord shows concentric bands of alternating demyelination and preserved myelin. **H.** CD68-positive macrophages are still abundant in the lesions. **I.** GFAP immunostaining indicates strong gliosis at the lesion edge and surrounding areas. **J.** AQP4 immunoreactivity is completely lost in the lesion center and the surrounding area with preserved myelin staining (note the AQP4-immunopositive area only at the periphery of the spinal cord). **K.** High magnification of the blood vessels indicated by the arrowhead in **I** and **J** shows numerous GFAP-positive reactive astrocytes and remnant astrocytic vascular foot processes. **L.** In the same area as **K**, AQP4 immunoreactivity is completely lost in the GFAP-positive structures. **A, G**, KB; **B, H**, CD68 immunohistochemistry (IHC); **C, E, I, K**, GFAP IHC; **D, F, J, L**, AQP4 IHC. Scale bar = 500 μm (**G–J**); 300 μm (**A–D**); 50 μm (**E, F**); 30 μm (**K, L**). AQP4 = aquaporin-4; GFAP = glial fibrillary acidic protein; KB = Klüver-Barrera staining; MS = multiple sclerosis.

demyelinating lesion. This represented 36% (4/11) of all NMO/NMOSD cases (Figure 7C). All of these cases demonstrated heterogeneity in the relationship between AQP4 loss and perivascular deposition of activated complement and immunoglobulins. Moreover, we also observed different patterns of AQP4 loss and perivascular deposition of activated complement and immunoglobulins even within a single lesion. For example, in NMO-10 with anti-AQP4 antibody, in the active cerebral lesions where AQP4 was totally lost, there was no deposition of either immunoglobulin or complement (Figure 5E–H). On the other hand, in the peripheral area of a chronic active demyelinating lesion (Pattern C) in the cerebral white matter, there were blood vessels surrounded by myelin showing variable degrees of diminished staining (Figure 6A). There was no macrophage infiltration or decreased AQP4 immunoreactivity in this area (Figure 6B, C), despite deposition of activated complement and immunoglobulins around some blood vessels (Figure 6D–G). Another chronic inactive lesion in the cerebral white matter, where AQP4 immunoreactivity was markedly increased (Figure 6H–J), showed perivascular deposits of activated complement and

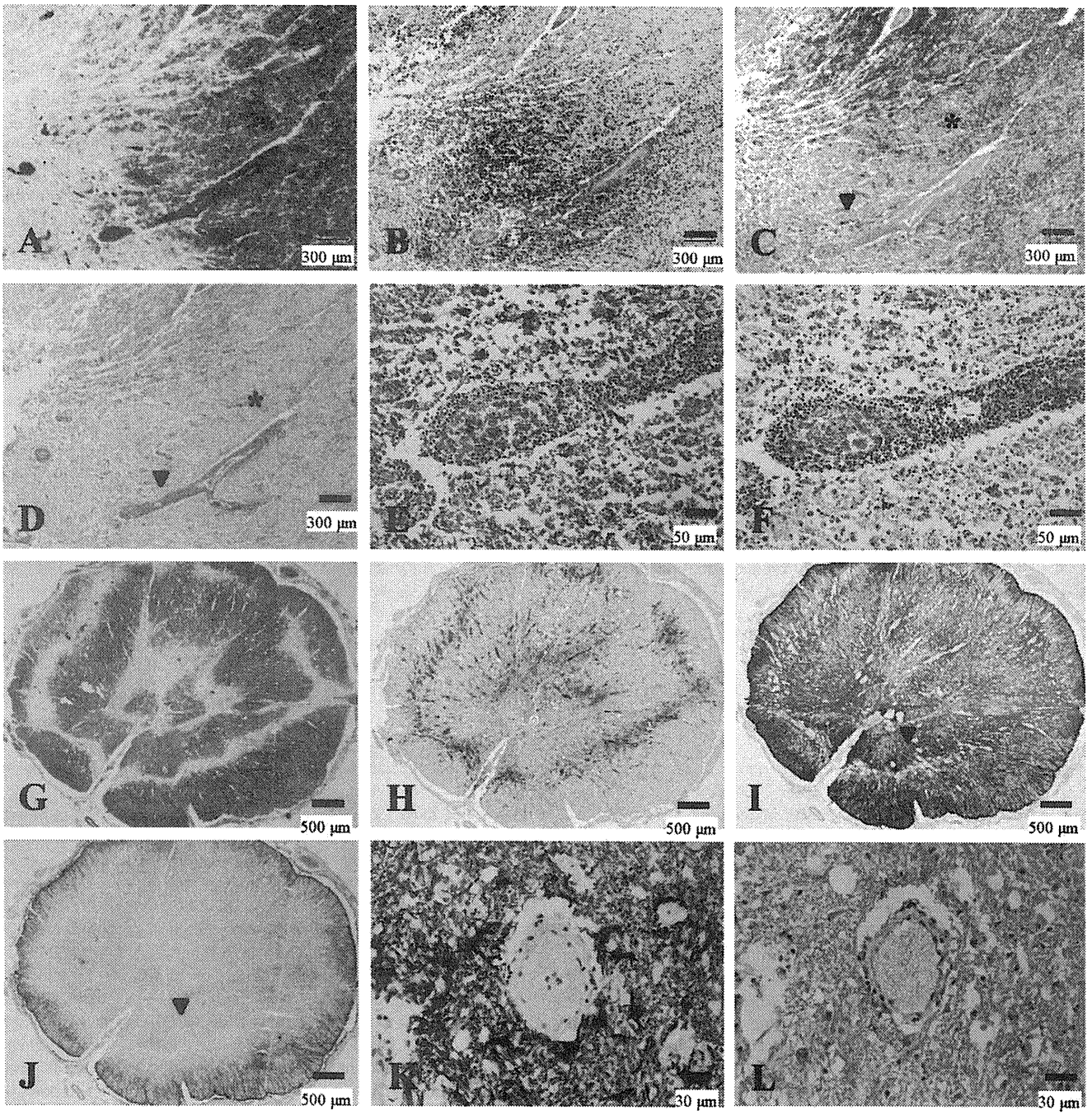

Table 6-1. Frequency of each aquaporin-4 immunoreactivity pattern in demyelinating lesions from cases with neuromyelitis optica (NMO) or NMO spectrum disorders. Abbreviations: NMO = neuromyelitis optica, NMOSD = neuromyelitis optica spectrum disorder.

Lesion pattern	NMO and NMOSD (n = 149)		
	Active (n = 42)	Chronic active (n = 72)	Chronic inactive (n = 35)
Pattern A	17	13	0
Pattern B	10	12	0
Pattern C	0	11	9
Pattern D	9	36	23
Pattern N	6	0	3

Table 6-2. Frequency of each aquaporin-4 immunoreactivity pattern in demyelinating lesions from cases with multiple sclerosis. Abbreviations: MS = multiple sclerosis.

Lesion pattern	MS (n = 51)		
	Active (n = 24)	Chronic active (n = 14)	Chronic inactive (n = 13)
Pattern A	4	4	0
Pattern B	7	3	0
Pattern C	0	1	1
Pattern D	7	6	12
Pattern N	6	0	0

See Table 3 for the definition of the patterns. Any pattern with necrosis (Patterns X and N) was included into Pattern X.

immunoglobulins (Figure 6K, L). However, chronic active lesions in the spinal cord demonstrated loss of AQP4 immunoreactivity with perivascular staining for complement and immunoglobulins (Figure 6M–O).

Areas with complement and immunoglobulin deposition, but without either demyelination or AQP4 loss (as shown in Figure 6B–G), were noted in five cases (three of the four NMO/NMOSD cases that showed concurrent perivascular complement and immunoglobulin deposition and AQP4 loss in some lesions, and one NMO/NMOSD case and one MS case that showed perivascular complement and immunoglobulin deposition, but neither AQP4 loss nor demyelination).

Relationship between perivascular lymphocytic cuffing and AQP4 loss

The frequency of each AQP4 expression pattern is summarized in Table 6. In actively demyelinating lesions, 23 of 38 (60.5%) Pattern A or B lesions (51.9% in NMO/NMOSD and 81.8% in MS) and eight of 16 (50.0%) Pattern D lesions (55.6% in NMO/NMOSD, and 42.9% in MS) showed perivascular lymphocytic cuffing. In total, perivascular cuffing was observed in 60% of the actively demyelinating lesions, regardless of clinical phenotype or AQP4 status (Figures 5K–M and 7B). In chronic active lesions, seven of 32 (21.9%) Pattern A or B lesions (16.0% in NMO/NMOSD and 42.9% in MS) and six of 42 (14.3%) Pattern D lesions (13.9% in NMO/NMOSD and 16.7% in MS) demonstrated perivascular lymphocytic cuffing. Generally, lymphocytic cuffing was milder in NMO/NMOSD than in MS. In addition, all lesions had predominant T-cell infiltration (30 in actively demyelinating lesions and 12 in chronic active lesions) (see Figure 5K–M).

DISCUSSION

We performed a systematic immunohistopathological study on autopsied cases of NMO and MS. Half of NMO patients showed preferential loss of AQP4 beyond the area of demyelination, whereas others did not, even in actively demyelinating lesions. Some MS patients, including one with only brain lesions and the other with BCS-like concentric spinal cord lesions, demonstrated extensive AQP4 loss in actively demyelinating and chronic active lesions, whereas other MS patients showed preservation of AQP4. Even NMO and MS patients with preferential AQP4 loss showed AQP4 patterns that varied from lesion to lesion, with no AQP4 loss in some of the actively demyelinating lesions, as well as in chronic active and inactive lesions. Vasculocentric deposition of complement and immunoglobulins was specifically noted in a third of NMO/NMOSD cases, but did not tightly correlate with perivascular AQP4 loss. Overall, our study indicates that antibody and

Figure 5. Distinctive patterns of perivascular immunoglobulin/complement deposition and lymphocytic cuffing between NMO and MS. **(A–D)** Active lesions in NMO with immunoglobulin/complement deposition. **(A, B)** Serial sections of a periplaque, still-myelinated area of NMO-4. These figures show the same area as that indicated by the arrowhead in Figure 1, G and I. IgM **(A)** and C3d **(B)** deposition are observed in astrocytic vascular foot processes as well as in degenerated astrocytes (arrowheads). **(C, D)** Serial sections from a more advanced active lesion in the spinal cord from NMO-7. IgG **(C)** and IgM **(D)** deposition are observed in astrocytic vascular foot processes as well as degenerated astrocytes (arrowheads). **(E–H)** Serial sections of an active lesion from NMO-10 without immunoglobulin/complement deposition. These figures show the periplaque, still-myelinated areas of the lesion shown in Figure 1A–F. Although GFAP immunoreactivity is preserved **(E)**, AQP4 expression is totally lost **(F)**. Neither C9neo **(G)** nor IgG **(H)** staining shows specific perivascular deposition. **(I, J)** Lack of immunoglobulin/complement deposition in MS. Serial sections of a chronic active lesion from MS-4. These figures show the same area as in Figure 4K and L. Neither IgG **(I)** nor C3d **(J)** staining shows typical perivascular deposition. **(K–M)** Lymphocyte cuffing in MS and NMO. **(K, L)** Serial sections from an active lesion from MS-3. These figures show the same lesion as in Figure 4E and F. **K.** CD45RO staining demonstrates perivascular cuffing predominantly consisting of T cells. **L.** Few CD20-positive B cells in the perivascular area. **M.** An active lesion in the spinal cord from NMO-7. This figure shows the same lesion as in **C** and **D**. Although CD45RO-positive T-cells predominate, the degree of perivascular lymphocyitic accumulation is much milder in NMO than in MS. **A, D**, IgM immunohistochemistry (IHC); **B, J**, C3d IHC; **C, H, I**, IgG IHC; **G**, C9neo IHC; **E**, GFAP IHC; **F**, AQP4 IHC; **K, M**, CD45RO IHC, **L**, CD20 IHC. Scale bar = 100 μm **(K, L)**; 50 μm **(A–J, M)**. AQP4 = aquaporin-4; GFAP = glial fibrillary acidic protein; KB = Klüver-Barrera staining; MS = multiple sclerosis; NMO = neuromyelitis optica.